



Polyaniline based magnesium nanoferrite composites as efficient photocatalysts for the photodegradation of Indigo Carmine in aqueous solutions

Asifa Bashir^a, Farzana Hanif^b, Ghazala Yasmeen^a, Fazal Mabood^c, Ahmad Hussain^d, Naseem Abbas^{a,*}, Ammar Bin Yousaf^e, Muhammad Aamir^a, Suryyia Manzoor^{a,*}

^aInstitute of Chemical Sciences, Bahuddin Zakariya University, Multan, Pakistan, Tel. 0092415985949, email: Asifabashir72@gmail.com (A. Bashir), Tel. 00923006345628, email: Ghazala31pk@yahoo.com (G. Yasmeen), Tel. 03009109435, email: dr.naseem.abbas@gmail.com (N. Abbas), Tel. 00923006372302, email: aamirmirza321@yahoo.com (M. Aamir), Tel. 00923339166673, email: Suryyia878@gmail.com (S. Manzoor)

^bGovernment Sadiq College Women University, Bahawalpur, Pakistan, Tel. 00923017745540, email: farzanawajid67@gmail.com (F. Hanif)

^cUniversity of Nizwa, Sultanate of Oman, Tel. 0096895971085, email: mehboob@unizwa.edu.om (F. Mabood)

^dShaheed Zulfiqar Ali Bhutto university of Science and Technology, Karachi, Pakistan, Tel. 00923232723411, email: ahmad.hussain@szabist.edu.pk (A. Hussain)

^eCentre for Advanced materials, Qatar University, Doha 2713, Qatar, Tel. 00923166916572, email: Ammar.chemist18@gmail.com (A.B. Yousaf)

Received 27 October 2017; Accepted 13 May 2019

ABSTRACT

The industrial revolution although has reached its unprecedented altitude benefiting mankind in various aspects yet the resulting pollution is a serious threat to the environment. Dyes are among the major pollutants that contaminate water resources. Hence, a facile synthesis of PANI/MgFe₂O₄ nanoferrite composite and its hybrids as photocatalysts for the degradation of Indigo carmine in aqueous solutions is described. The photocatalysts were designed in situ through self-polymerization of monomer aniline. The catalytic activity of each composite was studied by evaluating its efficiency to photodegrade water soluble carcinogenic indigo carmine dye in aqueous solution. Different parameters like dye concentration, dose of photocatalyst, contact time and pH have been studied to optimize reaction conditions. The FTIR, SEM and XRD studies were carried to determine chemical as well as morphological feature characteristics of nanoferrite composite (MgFe₂O₄+PANI) and hybrid nanoferrite composites (MgFe₂O₄ + PANI + silica gel). The XRD confirmed the cubic structure of nano ferrite. The SEM image of polyaniline/composite suggested porous surface and highly agglomerated granular shape. The FTIR spectra of polyaniline and its composites evinced the formation of composite possessing spinal ferrite structure. The single coated PANI/MgFe₂O₄ composite presented higher photo-degradation percentage i.e. 97.52% as compared to hybrid nanoferrite composites i.e. 94.36% and hence presented promising results to purify water contaminated with respective dye.

Keywords: Polyaniline; Polyaniline/magnesium nanoferrite composite; Hybrid nano-composites; Photodegradation

*Corresponding author.

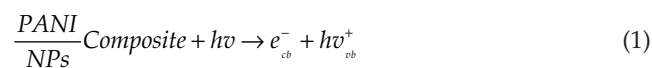
1. Introduction

An efficient photocatalytic process demands a sufficient and sustainable absorption of solar light. This can be achieved by implying a synthetic scheme that can result in the attaining of photocatalysts with low band gap. Ferrites are one of the facile approaches to such materials and their characteristics can be tuned by incorporating new moieties to their structure either through chemical means or by physical methods in order to enhance their desired properties [1–3]. They offer an advantage of being thermally and chemically stable magnetic materials. Hence, the process of doping has received considerable attention to introduce metal oxides and polymers for acquiring modified nanoferrite composites [4,5]. These materials have found vast applications in various fields especially for the photodegradation of drugs, dyes and other organic pollutants. Imprinting of specific template over these photocatalysts can result in the degradation of selective compounds. Following this approach, Lu et al. synthesized imprinted cobalt nanoferrites for the selective photodegradation of ciprofloxacin [6].

The principal goal for designing composites is to obtain distinctive properties in single material through integration of the compounds having required characteristics, therefore by combining the two properties like conductivity of polymers with the magnetic properties of the metal oxides; we can get the conducting polymers with magnetic properties [7–11].

Advanced techniques e.g. micro-encapsulation, electroplating, thermal spraying, flame spraying, physical vapour deposition (PVD), co-precipitation etc. for the coating of various polymers for the surface modification of nano ferrites have been successfully introduced [6,12,13]. The coating of the polyaniline (PANI) can provide the healing effects to make the surface of the nanoparticles smooth related to their surface defects, as the polyaniline provides the coating effects to the substances even which are in contact with the reaction mixture by forming the 100–200 nm thick film [14]. This fact makes polyaniline an appropriate polymer for the coating of ferrite [15] and is also explained by Lu et al. in microwave synthesis of TiO_2 for photodegradation study of enrofloxacin hydrochloride residues solution [16].

As these nanoferrite composites also exhibit excellent photocatalytic properties, therefore, can be employed for the purpose of water remediation due to their ability to degrade organic pollutants especially dyes [17–19]. The degradation mechanism involves the attack of hydroxyl radicals which are generated upon exposure to UV light in the presence of photocatalyst. The mechanism suggests the activation of the surface of the photocatalyst by UV light due to the excitation of electron from valence band to the conduction band leaving a hole. The water molecules interact with the electron and the hole to generate $\cdot\text{OH}$, OH^- and H^+ which cause the photodegradation reaction traps and making them available for the reactions occurring at the surface of photocatalyst and avert their recombination [20].



This work aims to synthesize the magnetic nanoferrites coated with the conducting polymer polyaniline, because in the family of intrinsically conducting polymers (ICPs), polyaniline is a salient member with potential electrical and magnetic as well as conductive properties. Therefore, doubly coated polyaniline nano-composites of silica gel and PANI/ferrite are reported in this work. The developed photocatalysts (nanoferrite coated with PANI and silica gel) were then applied for the photodegradation of dye Indigo carmine which is being extensively used in leather and textile tanning industries for many purposes like biological stain, antibacterial agent, additive to poultry feed and dermatological agent [21,22]. However, it is highly toxic to mammalian cells, recalcitrant and potent carcinogenic [23]. These effluents released from the textile and leather tanning industries impart color to the water thus making it non-potable for daily use.

The technology used to treat dyes is based on physical, chemical, and biological methods. Precipitation, coagulation, filtration, floatation, electrochemical degradation, and advanced oxidation techniques are considered as chemical methods [24]. Indigo carmine is an acidic dye and is called 5, 5'-indigodisulfonic acid sodium salt or indigotine [25].

In indigoid class of dyes, indigo carmine is highly toxic dye which causes eyes and skin irritation, and may also cause the permanent injury to conjunctiva or cornea. Consumption of the indigo carmine can lead to the developmental, reproductive or neural toxicity. Its use may also cause the gastrointestinal inflammation, nausea, vomiting, and diarrhea [26].

Therefore, the synthesis of such kind of novel photocatalysts with enhanced photodegradation ability can deem an efficient way to remove the dye from water, turning the procedure facile as well as cost effective.

2. Experimental

2.1. Reagents

Ammonium peroxy disulphate (98.0%) was purchased from DUKSAN, ferrous chloride (99.7%) ferric chloride (99%) were obtained from UNI-CHEM, magnesium chloride (98.5%), anilinium hydrochloride (99.0%), silica gel (99.0%), potassium dichromate (99.0%) were purchased from MERCK, Germany. Acetone (99.5%), Indigo carmine (96.0%), sulphuric acid (98.0%) from BDH, ammonia (25.0%) from Honeywell and potassium bromide (99.5%) was obtained from Riedel-de Haen, Germany. All these chemicals were used as such without further processing.

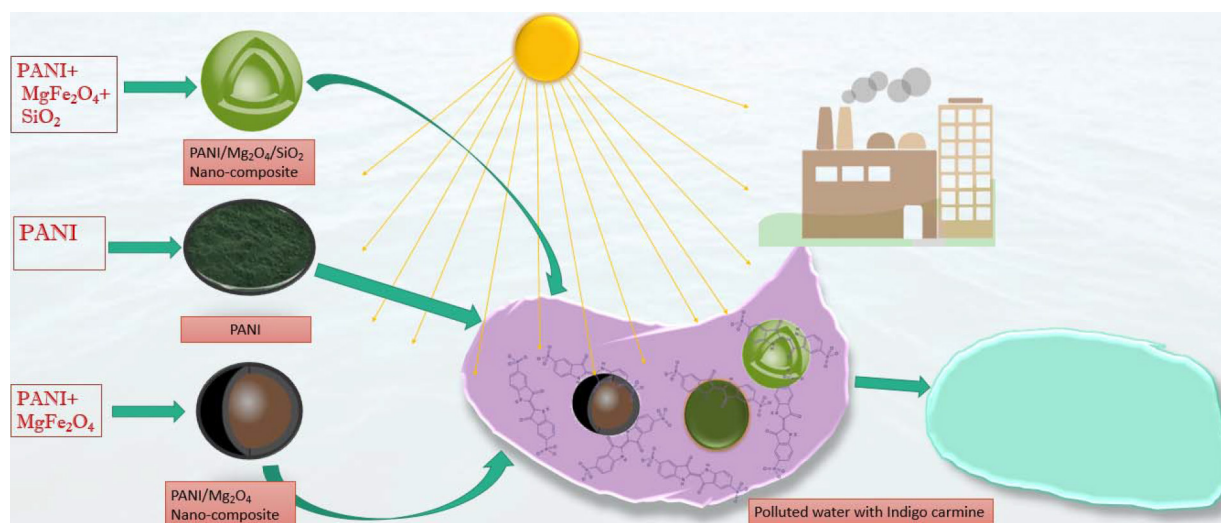


Fig. 1. Schematic representation of potential applications of synthesized nanoferrites.

2.2. Synthesis of nanoferrites

Nanoferrites were prepared by the co-precipitation method. Solutions of ferric chloride (0.4 M), ferrous chloride (0.1 M) and magnesium chloride (0.1 M) were mixed in a beaker (1000 mL) and heated at 100°C for half an hour, at constant stirring speed of 80 rpm. Then pH of the solution was adjusted to 10–11 by the drop wise addition of 2 M ammonia solution at a constant stirring speed of 140 rpm. This resulted in the formation of dark brown precipitates. After completion of the reaction, the precipitates were allowed to settle down for about 24 h. Mother liquor was removed from the sample solution by filtration. Sample was filtered with Whatman's (42 mm) filter paper. The obtained precipitates were washed with deionized water, until pH became neutral. The sample was dried at 100°C and ground to fine powder with the help of pestle and mortar. Prepared sample was stored in air tight bottle.

2.3 Synthesis of polyaniline

100 mL of aniline hydrochloride (0.2 M) solution was taken in a beaker and was stirred continuously at speed of 80 rpm. 100 mL ammonium peroxydisulphate (0.2 M) was added drop wise from the burette into the solution which resulted in the formation of blue green precipitates. Stirring was continued for 1 h even after the completion of the reaction. The solution was kept for 24 h for settling of precipitates. These precipitates were filtered with Whatman's (42 mm) filter paper and washed firstly with the deionized water and then with the acetone. Drying of precipitates was carried out at 60°C overnight. Finally the sample was ground to fine powder and stored.

2.4. Synthesis of core-shell nanoferrite composites

A typical in situ chemical polymerization reaction for the PANI/MgFe₂O₄ core shell nanocomposite was done by the routine synthesis [27]. Same procedure was repeated for

the synthesis of nanoferrite composites as used in section 2.3. The only difference is addition of anilinium hydrochloride solution in 0.1 g of the nanoferrite.

2.5. Synthesis of doubly coated nanoferrites

For the synthesis of hybrid nanoferrite-composites, the same procedure was repeated as mentioned in section 2.3. The nanoferrites and silica gel, both in equal amounts i.e. 0.1 g were added in 100 mL solution of anilinium hydrochloride (0.2 M). Solution was stirred for 10 min. Then 100 mL of freshly prepared ammonium peroxydisulphate solution (0.2 M) was added.

2.6. Parametric studies

Different analytical parameters were optimized to study the photodegradation of dyes using the three synthesized materials. i.e. polyaniline, single coated MgFe₂O₄ and doubly coated MgFe₂O₄ composites.

2.6.1. Preparation of dye solution

20 mg/L stock solution of the dye was prepared by dissolving 20 mg of the dye in 1 L of the deionized water. This solution was shaken well and stored in dark place. Further dilution of the dye solution (1 mg/L, 2 mg/L, 3 mg/L, 4 mg/L) was made from the stock solution as necessary. The experiment was performed by scanning the appropriate wavelength of indigo carmine dye at 608 nm.

A photodegradation study was carried out on the dye to check the efficiency of the prepared sample in the UV reactor which consists of a UV lamp. It is basically the study of degradation of the dyes in the presence of ultra-violet radiations with the help of suitable catalyst. Prior to irradiation, catalyst and dye solution mixture was stirred for about 15 min. A magnetic stirrer was used in this method to ensure the uniform mixing of the sample. Four parameters i.e. optimization of dye concentration, catalytic dose, time

and pH were studied using prepared samples (pure polyaniline, ferrite composites, doubly coated sample).

Percentage of dye degradation dye was estimated by following formula [28]:

$$\text{Photodegradation rate (\%)} = \frac{(C_o - C)}{C_o} \times 100 \quad (7)$$

where C_o is the initial concentration of the dye solution (before degradation) and C is the final concentration (after degradation).

2.6.2. Optimization of concentration of dye

Initial concentration of the dye solution was varied from 1–4 mg/L. 50 mL of each dye solution was taken in a beaker and 0.1 g of the catalytic sample was added in it and before irradiation, mixture was stirred on magnetic stirrer. Then sample was irradiated by U.V radiations. 5 mL aliquots of the sample were taken from the solution after every 10 min and their absorbance was noted by U.V spectrophotometer at λ_{max} 608.

2.6.3. Optimization of catalytic dose

In photocatalytic study, catalytic dose is an important parameter that is extensively studied. The catalytic activity of the sample material was calculated by changing the amount of the catalyst from 0.05–0.25 g by keeping the concentration of dye solution constant. 50 mL of the 4 mg/L dye solution was taken in a beaker and 0.05 g of the sample was added in it. Sample was stirred for about 15 min and kept in UV light. 5 mL of the aliquots were taken from the sample at regular time intervals and the absorbance was measured using the UV/visible spectrophotometer.

2.6.4. Optimization of time

Time is the major factor which influences the rate of photocatalytic phenomenon. Optimized time is required to attain efficient photodegradation activity. In order to study the influence of the time on photodegradation of dye, 50 mL of dye solution was taken in a beaker; optimized amount of the sample dose showing maximum activity was added in the solution and stirring was carried out for 15 min. The resulting mixture was then kept under UV light in a photoreactor. Experiment was carried out for about 60 min., aliquots were taken at regular intervals of 10 min from the reactor and absorbance was determined by UV/visible spectrophotometer.

2.6.5. Optimization of pH

The effect of pH was studied in the range of 1–14. The pH of the solutions was adjusted by adding sulphuric acid (2 M) or NaOH (2 M). 50 mL of the optimized dye solution was taken in a beaker and optimized catalytic dose was added in it. The sample mixture was stirred for 15 min and UV/visible was irradiated for 10 min. Absorbance of dye solution was then noted at each pH. The same procedure

was followed to optimize the conditions of analysis for the three synthesized materials.

2.6.6. Stability studies

Stability studies were performed using the procedure described in the literature [29]. The FT-IR spectrum of the photocatalyst was taken before use and then was run for 5 cycles. The photocatalyst was washed and dried before applying for the next cycle. The FT-IR spectrum was then taken after 5 runs. Moreover, the percentage degradation of the dye was measured for the five consecutive cycles.

3. Results and discussion

Ferrites are the compounds which are generally composed of the combination of iron oxide (Fe_2O_3) with metals [30] and both are ferrimagnetic and non-conducting. The general chemical formula of the simple ferrites is MeFe_2O_4 where Me represents the divalent metal ion with ionic radius of 0.6–1 Å and Me is the divalent metal ion of transition metal elements Mn, Co, Ni, Zn, Cu, Mg, Cd [31–34]. Other trivalent cations like Al^{3+} or Cr^{3+} can replace the trivalent ferric ions Fe^{3+} partly or completely giving rise to the mixed crystals with aluminates and chromates respectively.

In the present study polyaniline (PANI), PANI/ MgFe_2O_4 nanoferrite composite and PANI/ MgFe_2O_4 coated with silica samples are prepared by co-precipitation method. These samples have been characterized by FTIR technique. The PANI/ MgFe_2O_4 nanoferrite composite presented the highest photodegradation efficiency and hence were further characterized using XRD and SEM-EDS techniques. Then a photodegradation study of Indigo carmine has been carried out with these synthesized samples.

3.1. FTIR analysis

The FTIR spectroscopy was used to identify the functional groups present in (PANI), PANI/ MgFe_2O_4 nano ferrite composite and PANI/ MgFe_2O_4 coated with silica samples. FTIR studies were carried out by FTIR 400 SHIMADZU. The prepared samples were characterized in the range of 650–4000 cm^{-1} (Fig. 2). The FTIR spectra clearly show the formation of composite. In the latter, the characteristic bands of PANI appeared and shifted to the lower wavenumber. The characteristic main bands of PANI are assigned at 827 cm^{-1} , 860 cm^{-1} , 1190 cm^{-1} , 1361 cm^{-1} , 1507 cm^{-1} , 1627 cm^{-1} , 2030 cm^{-1} . In case of polyaniline, the band at 827 cm^{-1} attributes to the para-substituted aromatic rings showing polymer formation. The band below 860 cm^{-1} represents the aromatic C-H out-of plane bending vibrations and at 1190 cm^{-1} represents the C-H in-plane bending vibrations. The band at 1361 cm^{-1} is typical for the emeraldine base, attributed to the C-N stretching vibrations in the neighborhood of a quinoid ring and at 1507 cm^{-1} is due to the benzenoid ring stretching. The band at 1627 cm^{-1} represents the Aryl substituted C=C bond. It is characteristic for the polymers and above 2000 cm^{-1} is due to the absorption of the free charge-carriers in the protonated polymer. It is characteristic for the conducting polymer (polyaniline) [35].

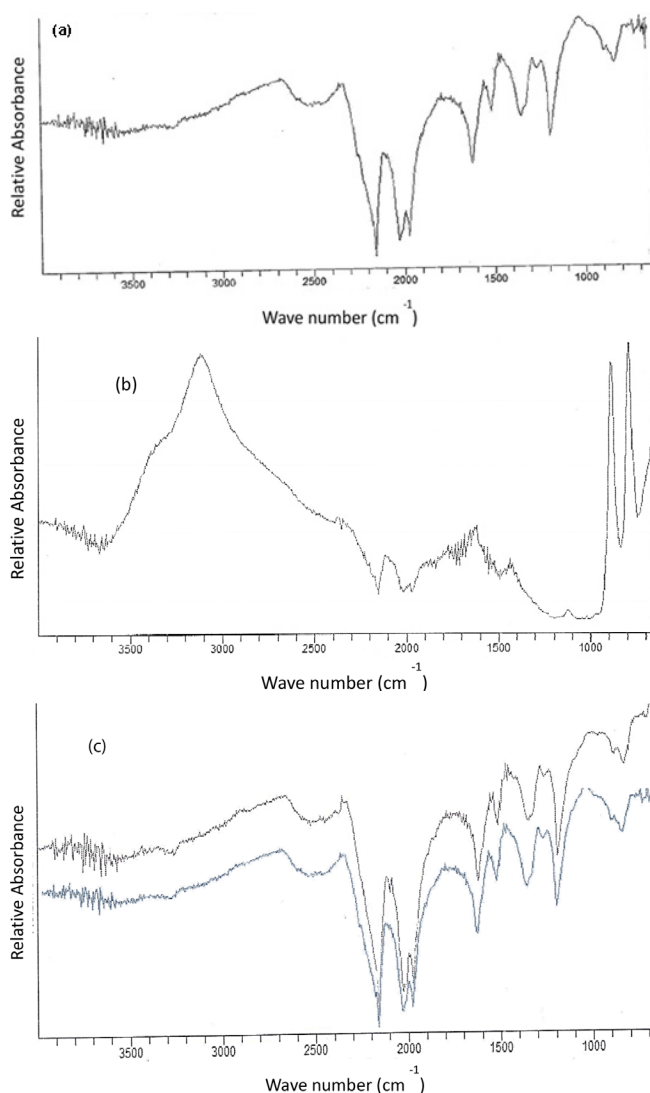


Fig. 2. FTIR spectra of (a) PANI, (b) MgFe_2O_4 , (c) PANI/ MgFe_2O_4 (black) and PANI/ MgFe_2O_4 /Silica (blue).

In MgFe_2O_4 , generally the metal oxide vibrations occur below 1000 cm^{-1} . The peaks appearing around 700 cm^{-1} are due to the spinel structure of the ferrites. The peak at the 3660 cm^{-1} represents the presence of the -OH group in the sample.

The FTIR spectrum of the silica, region of $1200\text{--}1000\text{ cm}^{-1}$ represents the intense silicon-oxygen covalent bonds vibrations, revealing the existence of a dense silica network, in which the oxygen atoms play role of bridges between two silicon sites. The broad and intense band appearing at 1090 cm^{-1} and the shoulder at around 1200 cm^{-1} are due to the transversal optical and longitudinal optical modes of the Si-O-Si asymmetric stretching vibrations. The symmetric stretching vibrations of Si-O-Si are present in the spectrum at 800 cm^{-1} . Their bending modes appear on $496\text{--}467\text{ cm}^{-1}$ [36].

The characteristic bands of PANI and MgFe_2O_4 were observed in the spectrum of single coated photocatalyst (PANI/ MgFe_2O_4) while in case of double coated photocatalyst (hybrid-nano-composite: PANI/ MgFe_2O_4 /Silica),

the silica band was also observed along with the other two above mentioned bands which confirm the successful synthesis of both nanoferrite-composites.

3.2. XRD analysis

The structural study of photocatalysts was carried out using X-Ray Diffraction analysis with the help of Philips X Pert PRO 3040/60 diffractometer. XRD patterns are given in Fig. 3.

The technique was used to examine the crystallite size, lattice constant, cell volume of the as synthesized PANI, PANI/ MgFe_2O_4 nanocomposites. The XRD pattern presents the peaks with the reference pattern of PANI and MgFe_2O_4 (00-053-1717) (00-010-0325) which confirms the successful synthesis of the nanocomposite with cubic structure. The particle size was calculated to be 47 nm using Scherer's equation. The XRD data was employed to study cell constant with approximate value, \AA which is in agreement with the reference pattern.

3.3. SEM/EDS analysis

The surface morphology and elemental composition were studied by SEM/EDS analysis. SEM images of MgFe_2O_4 and PANI/ MgFe_2O_4 are shown in Fig. 4. The SEM images clearly present a difference in the morphology of the materials. The SEM image of MgFe_2O_4 shows some small and less agglomerated particles as compared to PANI/ MgFe_2O_4 nanoferrite composite which are highly agglomerated granular in shape and has amorphous nature. The EDS analysis was populated and results are presented as mass % of the elements (Tables 1 and 2). The presence of higher carbon mass in case of PANI/ MgFe_2O_4 confirms the coating of the particles.

3.4. Parametric studies

Photodegradation study of Indigo carmine dye is carried out with PANI, PANI/ MgFe_2O_4 and PANI/ MgFe_2O_4 /silica coated samples. The process is optimized at conditions such as time, catalytic dose, concentration and pH.

The photocatalytic degradation of Indigo carmine dye was studied at $\lambda_{\text{max}} 608\text{ nm}$ to check the maximum photo-degradation with four parameters given below:

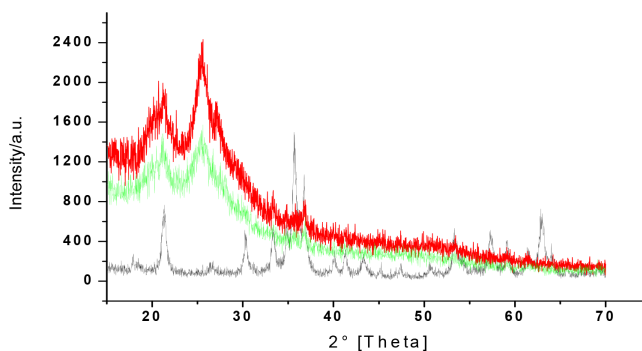


Fig. 3. XRD Pattern for MgFe_2O_4 (black), PANI/ MgFe_2O_4 (red), PANI/ MgFe_2O_4 /Silica (green).

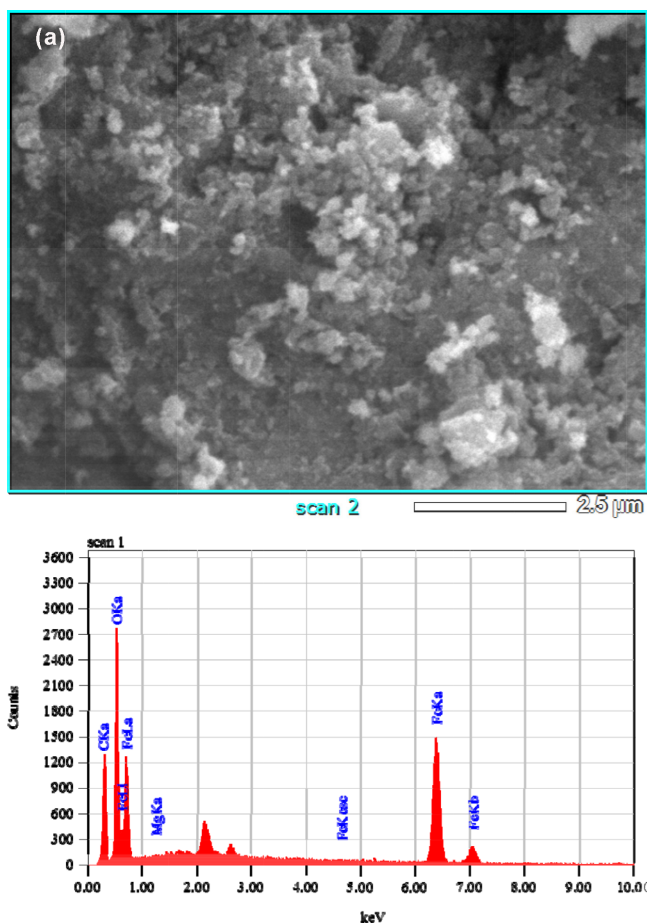


Fig. 4a. SEM/EDS analysis of $MgFe_2O_4$.

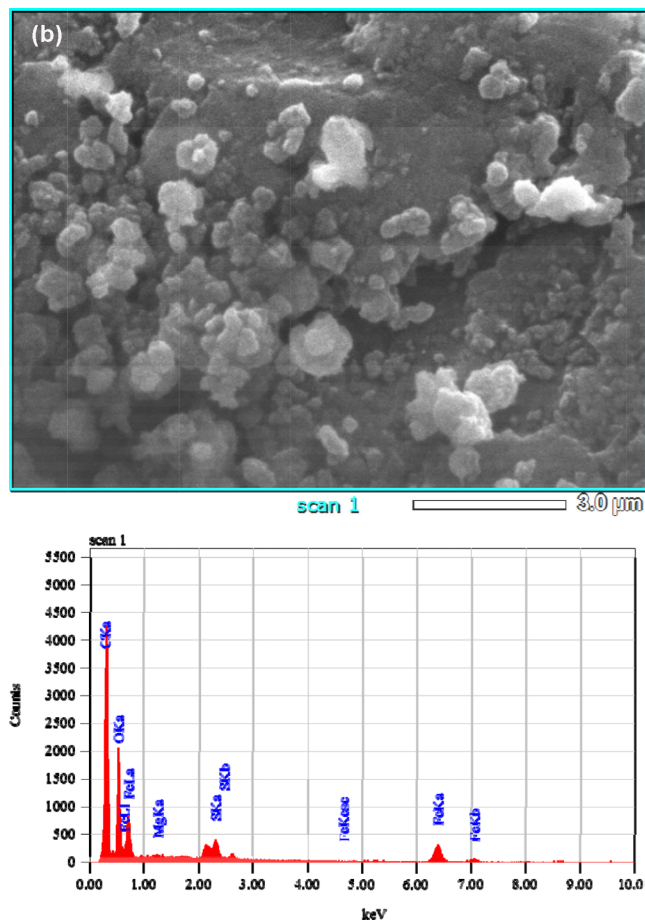


Fig. 4b. SEM/EDS analysis of $PANI/MgFe_2O_4$.

3.4.1. Concentration effect

Concentration of the dye present in the effluent water is the major factor causing problems in the aquatic life. Therefore effective concentration of the dye solution was examined to evaluate maximum capacity of photocatalysts to degrade dye. The effect of concentration is shown in Figs. 5–7 and it is observed that by increasing the concentration of the dye, photodegradation activity increases and is maximum in the case of polyaniline as catalyst which is about 92.08 %, after polyaniline it is observed that the singly coated sample shows good results than doubly coated sample, 88.07% and 86.25 % respectively. At the low dye concentration, the number of the active charge carriers is low on the surface of the conducting polymer, therefore by increasing the concentration of the dye, catalyst surface occupied with dye molecules so it increase the concentration degradation rate.

3.4.2. Effect of dose of catalyst

Effect of catalyst dose is shown in Figs. 8–10 for the photodegradation of the indigo carmine dye with polyaniline and its nanocomposites. Just like the optimization of the dye concentration, the effect of catalytic dose for the all three composites is different. It is observed that the photodegradation is maximum in the case of $PANI/MgFe_2O_4$

(0.05 g) about 97.52%, then 94.36% with $PANI/MgFe_2O_4$ /silica (0.20 g) and least in the case of polyaniline (0.15 g) about 92.43%. It means that for photodegradation activity with respect to catalytic dose, $PANI/MgFe_2O_4$ /silica nanocomposites are affective materials which are actually a good effort to clear the wastewater of many industries.

3.4.3. Contact time

The effect of time is shown in Figs. 11–13 for indigo carmine dye with prepared samples. It is observed that photocatalytic degradation is maximum in the case of polyaniline i.e. 99.15 % after 20 min. $PANI/MgFe_2O_4$ pre-

Table 1
Mass % of different elements in $MgFe_2O_4$

Element	C	O	Mg	Fe
Mass %	7.53	23.13	0.06	69.28

Table 2
Mass % of different elements in $PANI/MgFe_2O_4$

Element	C	O	Mg	Fe	S
Mass %	30.91	41.29	0.22	24.40	3.19

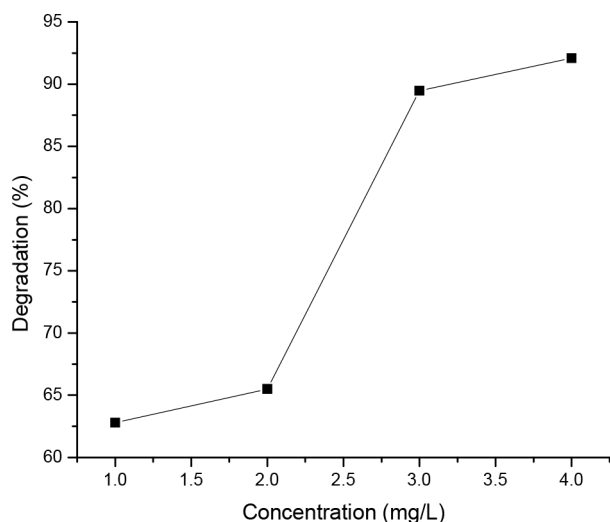


Fig. 5. Photodegradation(%) as function of concentration of dye (indigo carmine) with pure PANI sample.

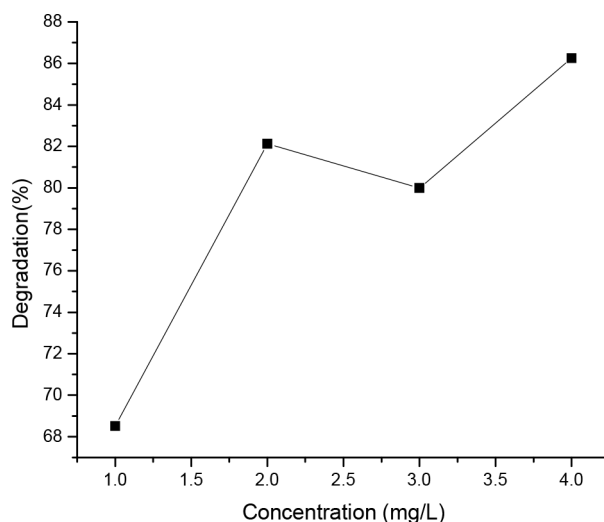


Fig. 7. Degradation (%) as function of concentration of dye (indigo carmine) with PANI/MgFe₂O₄-silica coated composites.

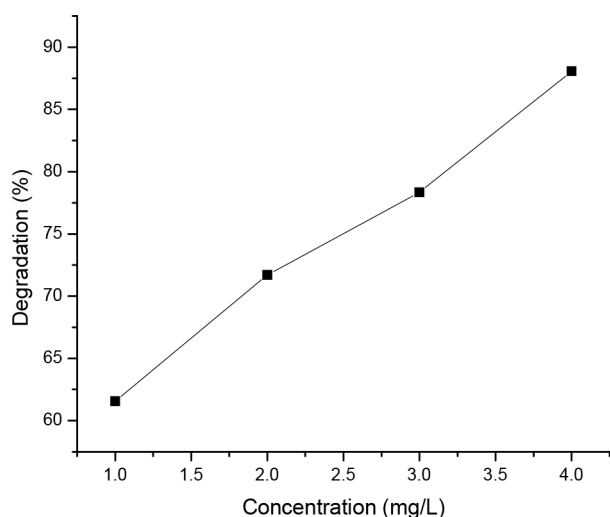


Fig. 6. Degradation (%) as function of concentration of dye (indigo carmine) with PANI/MgFe₂O₄ composites.

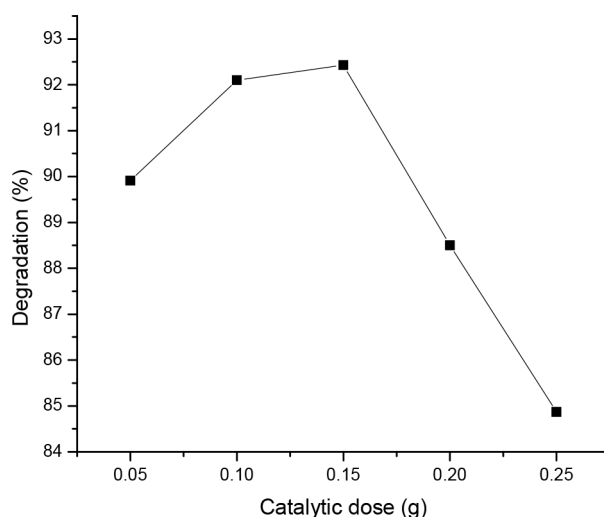


Fig. 8. Percent degradation of indigo carmine dye as a function of catalytic dose of pure PANI sample.

sented a photocatalytic activity of 92.58 after 10 min and 91.93% is obtained in the case PANI/MgFe₂O₄/silica at 60 min. Initially surface of photocatalyst is not efficiently activated therefore catalytic activity is slow but as the photocatalyst surface gets activated, rate of degradation increases rapidly. As the maximum concentration of dye is degraded from aqueous solution, the rate of degradation reaches at equilibrium.

3.4.4. pH effect

The analysis of the role of pH on the efficiency of the photodegradation process is a strenuous task. This is because three possible reaction mechanisms can contribute to dye degradation, (1) hydroxyl radical attack, (2) direct oxidation by the positive hole, and (3) direct reduction by the electron in the conducting band. The contribution of each one depends on the substrate's nature and pH. The

pH of the solution modifies the electrical double layer of the solid electrolyte interface, and consequently affects the sorption–desorption processes and the separation of the photogenerated electron–hole pairs in the surface of catalysts [37].

The effect of pH is shown in Figs. 14–16 for indigo carmine dye with PANI and its composites. Photodegradation is maximum with PANI/MgFe₂O₄ composites i.e. 96.14 % at pH 2, then with PANI/MgFe₂O₄/Silica 95.35% at pH 2 and least in the case of pure polyaniline 90.69% at pH 13.

The optimum conditions for the removal of the indigo carmine dye after parametric optimization are initial concentration 4 mg/L with polyaniline (92.08 %), photocatalyst dose 0.05 g with PANI/MgFe₂O₄ (97.52%), time 20 min with polyaniline (99.15%) and pH 2 with PANI/MgFe₂O₄ (96.14 %).

The stability studies did not present prominent change in the FT-IR spectra of photocatalyst before and after use

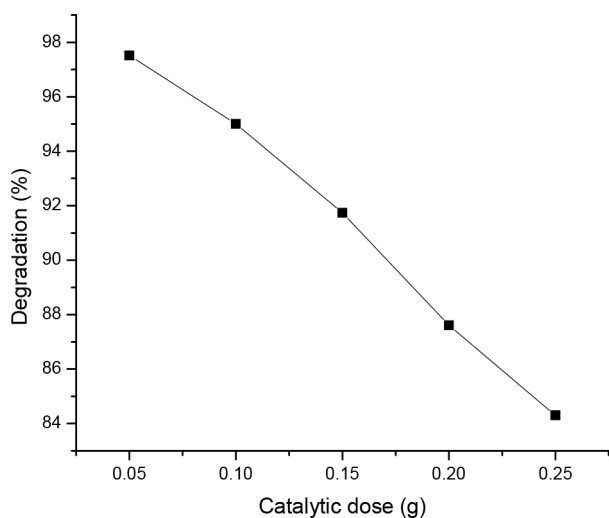


Fig. 9. Percent degradation of indigo carmine dye as a function of catalytic dose of PANI/MgFe₂O₄ sample.

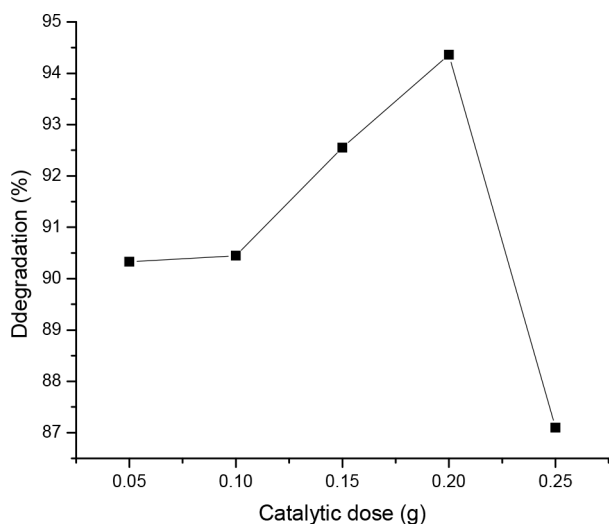


Fig. 10. Percent degradation of indigo carmine dye as a function of catalytic dose of PANI/MgFe₂O₄/silica coated composites.

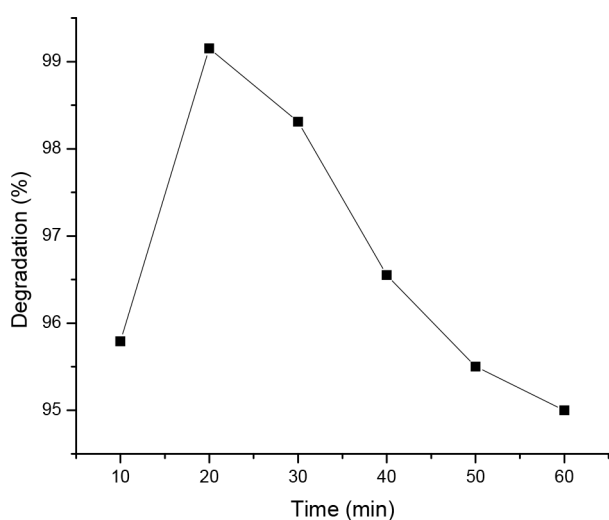


Fig. 11. Percent degradation of indigo carmine dye as a function of time with pure PANI sample.

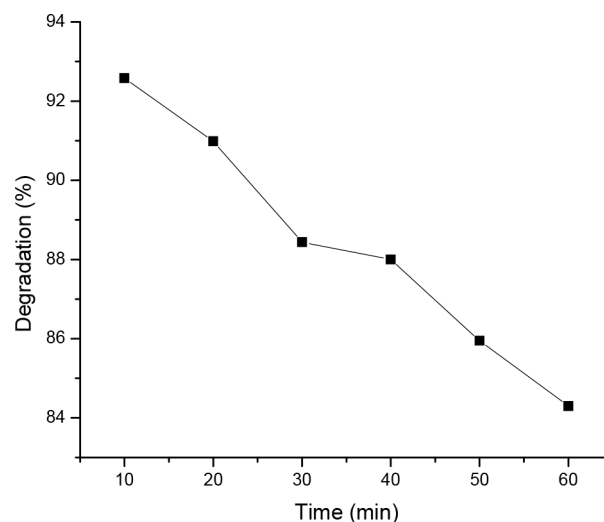


Fig. 12. Percent degradation of indigo carmine dye as a function of time with PANI/MgFe₂O₄ sample.

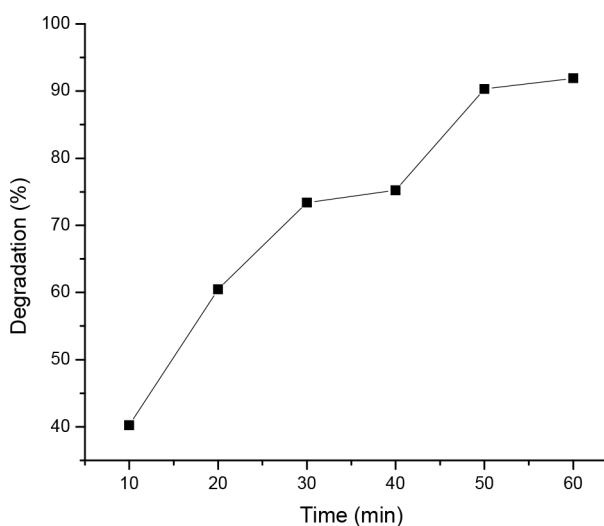


Fig. 13. Percent degradation of indigo carmine dye as a function of time with PANI/MgFe₂O₄/silica coated sample.

which suggests that the catalyst's structure hasn't undergone structural variation during the repetitive cycles. Similarly, the percentage photodegradation of the dye in five cycles varied between a narrow range of 96.5–98% with a RSD 0.63% and hence the photodegradation ability was not affected by its reuse.

4. Conclusion

PANI, PANI/MgFe₂O₄ and PANI/MgFe₂O₄ coated with silica composites are prepared by the oxidation of aniline chloride in the presence of NPs by ammonium peroxydisulphate via co-precipitation method. Results obtained by FTIR, XRD and SEM are comparable as given in literature. It is observed that photocatalytic degradation by PANI/MgFe₂O₄ is a more effective and faster mode of removing dyes as compared to the other materials studied in this

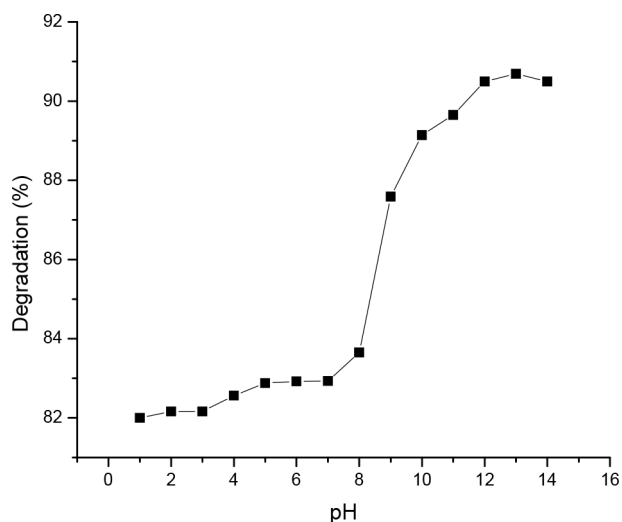


Fig. 14. Percent degradation of indigo carmine dye as a function of pH with pure PANI sample.

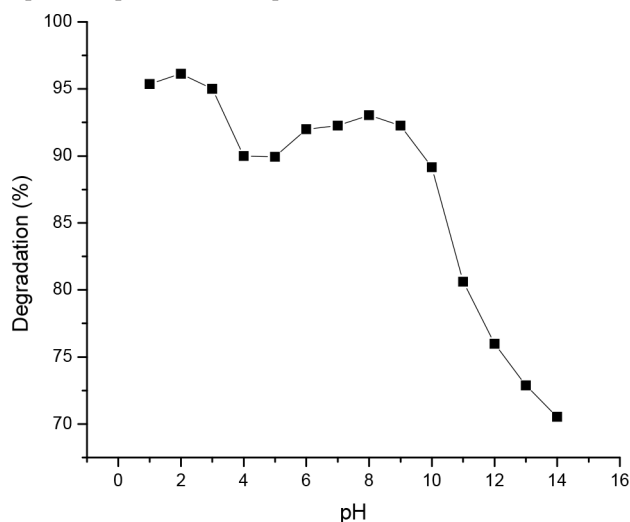


Fig. 15. Percent degradation of indigo carmine dye as a function of pH with PANI/MgFe₂O₄ sample.

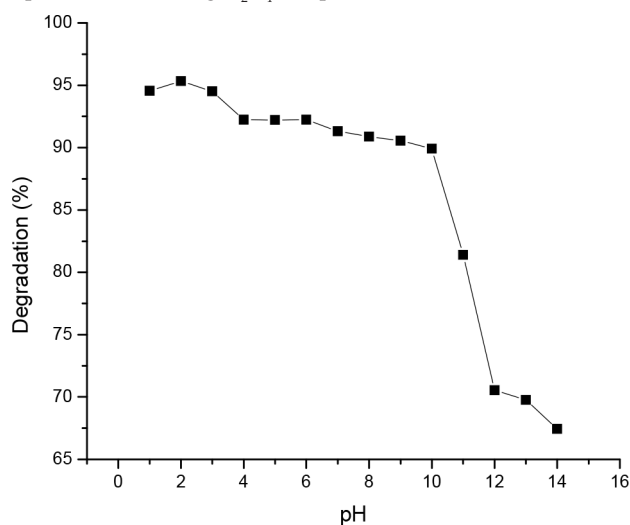


Fig. 16. Percent degradation of indigo carmine dye as a function of pH with PANI/MgFe₂O₄/silica coated sample.

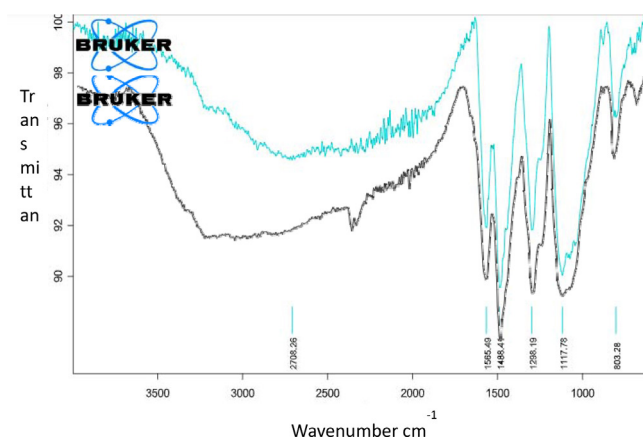


Fig. 17. FT-IR spectra of PANI/MgFe₂O₄ original sample before applying as photocatalyst (blue) and after five runs as photocatalyst (black).

work. Its catalytic dose of 0.05 g was sufficient to degrade 4 mg/L of the dye. The FTIR, XRD and SEM-EDS studies are carried for morphological and elemental feature characteristics of PANI-MgFe₂O₄ coated nanoferrite-composite.

The present study shows that conducting PANI/MgFe₂O₄ can be used as photocatalyst for the degradation of indigo carmine dye from aqueous solution.

References

- [1] E.E. Ateia, F.S. Soliman, Modification of Co/Cu nanoferrites properties via Gd³⁺/Er³⁺ doping, *Appl. Phys. A.*, 123 (2017) 312.
- [2] P. Majewski, P. Krysiński, Synthesis, surface modifications, and size-sorting of mixed nickel–zinc ferrite colloidal magnetic nanoparticles, *Chemistry - Eur. J.*, 14 (2008) 7961–7968.
- [3] D. Nieciecka, K. Nawara, K. Kijewska, A.M. Nowicka, M. Mazur, P. Krysiński, Solid-core and hollow magnetic nanostructures: Synthesis, surface modifications and biological applications, *Bioelectrochemistry*, 93 (2013) 2–14.
- [4] V.A. Kolesov, C. Fuentes-Hernandez, W.-F. Chou, N. Aizawa, F.A. Larrain, M. Wang, A. Perrotta, S. Choi, S. Graham, G.C. Bazan, Solution-based electrical doping of semi conducting polymer films over a limited depth, *Nature Mater.*, 16 (2017) 474–480.
- [5] H. Anwar, A. Maqsood, Comparison of structural and electrical properties of Co²⁺ doped Mn-Zn soft nano ferrites prepared via coprecipitation and hydrothermal methods, *Mater. Res. Bull.*, 49 (2014) 426–433.
- [6] Z. Lu, Z. Yu, J. Dong, M. Song, Y. Liu, X. Liu, D. Fan, Z. Ma, Y. Yan, P. Huo, Construction of stable core–shell imprinted Ag-(poly-o-phenylenediamine)/CoFe₂O₄ photocatalyst endowed with the specific recognition capability for selective photodegradation of ciprofloxacin, *RSC Adv.*, 7 (2017) 48894–48903.
- [7] D. Baeriswyl, D. Campbell, G. Clark, G. Harbeke, P. Kahol, H. Kiess, S. Mazumdar, M. Mehring, W. Rehwald, *Conjugated Conducting Polymers*, Springer Science & Business Media, 2012.
- [8] G. Zotti, G. Schiavon, S. Zecchin, J.-F. Morin, M. Leclerc, Electrochemical, conductive, and magnetic properties of 2, 7-carbazole-based conjugated polymers, *Macromolecules*, 35 (2002) 2122–2128.
- [9] H. Kim, B. Sohn, W. Lee, J.-K. Lee, S. Choi, S. Kwon, Multi-functional layer-by-layer self-assembly of conducting polymers and magnetic nanoparticles, *Thin Solid Films*, 419 (2002) 173–177.

- [10] R. Gangopadhyay, A. De, Conducting polymer nanocomposites: a brief overview, *Chem. Mater.*, 12 (2000) 608–622.
- [11] R.M. Khafagy, Synthesis, characterization, magnetic and electrical properties of the novel conductive and magnetic polyaniline/MgFe₂O₄ nanocomposite having the core-shell structure, *J. Alloys Comp.*, 509 (2011) 9849–9857.
- [12] R. Asapu, N. Claes, S. Bals, S. Denys, C. Detavernier, S. Lenaerts, S.W. Verbruggen, Silver-polymer core-shell nanoparticles for ultra stable plasmon-enhanced photocatalysis, *Appl. Catal. B: Environ.*, 200 (2017) 31–38.
- [13] Y. Wang, B. Sun, J. Park, W.-S. Kim, H.-S. Kim, G. Wang, Morphology control and electrochemical properties of nanosize LiFePO₄ cathode material synthesized by co-precipitation combined with in situ polymerization, *J. Alloys Comp.*, 509 (2011) 1040–1044.
- [14] N.E. Kazantseva, J. Vilčáková, V. Křesálek, P. Saha, I. Sapurina, J. Stejskal, Magnetic behaviour of composites containing polyaniline-coated manganese-zinc ferrite, *J. Magn. Magn. Mater.*, 269 (2004) 30–37.
- [15] L. Li, C. Xiang, X. Liang, B. Hao, Zn_{0.6}Cu_{0.4}Cr_{0.5}Fe_{1.46}Sm_{0.04}O ferrite and its nanocomposites with polyaniline and polypyrrole: preparation and electromagnetic properties, *Synth. Metals*, 160 (2010) 28–34.
- [16] Z. Lu, F. Chen, M. He, M. Song, Z. Ma, W. Shi, Y. Yan, J. Lan, F. Li, P. Xiao, Microwave synthesis of a novel magnetic imprinted TiO₂ photocatalyst with excellent transparency for selective photodegradation of enrofloxacin hydrochloride residues solution, *Chem. Eng. J.*, 249 (2014) 15–26.
- [17] S. Bhukal, S. Bansal, S. Singhal, Magnetic Mn substituted cobalt zinc ferrite systems: structural, electrical and magnetic properties and their role in photo-catalytic degradation of methyl orange azo dye, *Physica B: Condensed Matter*, 445 (2014) 48–55.
- [18] S. Bhukal, M. Dhiman, S. Bansal, M.K. Tripathi, S. Singhal, Substituted Co–Cu–Zn nanoferrites: synthesis, fundamental and redox catalytic properties for the degradation of methyl orange, *RSC Adv.*, 6 (2016) 1360–1375.
- [19] H. Assi, S. Atiq, S.M. Rammay, N.S. Alzayed, M. Saleem, S. Riaz, S. Naseem, Substituted Mg–Co-nanoferrite: recyclable magnetic photocatalyst for the reduction of methylene blue and degradation of toxic dyes, *J. Mater. Sci.: Mater. Electron.*, 28 (2017) 2250–2256.
- [20] M. Aamir, M.N. Ashiq, G. Yasmeen, B. Ahmad, M. Fahad Ehsan, T. He, Synthesis and characterization of polyaniline/Zr-Co-substituted nickel ferrite (NiFe_{1.2}Zr_{0.4}Co_{0.4}O₄) nanocomposites: their application for the photodegradation of methylene blue, *Desal. Water Treat.*, 57 (2016) 12168–12177.
- [21] R.S. N'Dri, M. Coulibaly, A.N.G. Yao, D. Bamba, E.G. Zoro, An electrochemical method for the determination of trace mercury (II) by formation of complexes with indigo carmine food dye and its analytical application, *Int. J. Electrochem. Sci.*, 11 (2016) 5342–5350.
- [22] S. Gopi, P. Balakrishnan, A. Pius, S. Thomas, Chitin nanowhisker (ChNW)-functionalized electrospun PVDF membrane for enhanced removal of Indigo carmine, *Carbohydr. Polym.*, 165 (2017) 115–122.
- [23] P.C.G. Pereira, R.V. Reimão, T. Pavesi, E.M. Saggioro, J.C. Moreira, F.V. Correia, Lethal and sub-lethal evaluation of Indigo Carmine dye and byproducts after TiO₂ photocatalysis in the immune system of Eisenia andrei earthworms, *Ecotoxicol. Environ. Safety*, 143 (2017) 275–282.
- [24] T.N. Ramesh, V.P. Sreenivasa, Removal of indigo carmine dye from aqueous solution using magnesium hydroxide as an adsorbent, *J. Mater.*, 2015 (2015) 10.
- [25] M. de Keijzer, M.R. van Bommel, R.H.-d. Keijzer, R. Knaller, E. Oberhumer, Indigo carmine: Understanding a problematic blue dye, *Stud. Conserv.*, 57 (2012) S87–S95.
- [26] N. Barka, A. Assabbane, A. Nounah, Y.A. Ichou, Photocatalytic degradation of indigo carmine in aqueous solution by TiO₂-coated non-woven fibres, *J. Hazard. Mater.*, 152 (2008) 1054–1059.
- [27] J. Jiang, L. Li, F. Xu, Polyaniline–LiNi ferrite core-shell composite: Preparation, characterization and properties, *Mater. Sci. Eng.*, (2007) 300–304.
- [28] Z. Lu, Z. Yu, J. Dong, M. Song, Y. Liu, X. Liu, Z. Ma, H. Su, Y. Yan, P. Huo, Facile microwave synthesis of a Z-scheme imprinted ZnFe₂O₄/Ag/PEDOT with the specific recognition ability towards improving photocatalytic activity and selectivity for tetracycline, *Chem. Eng. J.*, 337 (2018) 228–241.
- [29] Z. Lu, X. Zhao, Z. Zhu, Y. Yan, W. Shi, H. Dong, Z. Ma, N. Gao, Y. Wang, H. Huang, Enhanced re-cyclability, stability, and selectivity of CdS/C@Fe₃O₄ nanoreactors for orientation photodegradation of ciprofloxacin, *Chem.-Eur. J.*, 21 (2015) 18528–18533.
- [30] S. Stewart, S. Figueroa, M. Sturla, R. Scorzelli, F. García, F. Requejo, Magnetic ZnFe₂O₄ nanoferrites studied by X-ray magnetic circular dichroism and Mössbauer spectroscopy, *Physica B: Condensed Matter*, 389 (2007) 155–158.
- [31] U. Lima, M. Nasar, R. Nasar, M. Rezende, J. Araújo, Ni–Zn nanoferrite for radar-absorbing material, *J. Magn. Magn. Mater.*, 320 (2008) 1666–1670.
- [32] A. Salunkhe, V. Khot, M. Phadatar, N. Thorat, R. Joshi, H. Yadav, S. Pawar, Low temperature combustion synthesis and magneto structural properties of Co–Mn nanoferrites, *J. Magn. Magn. Mater.*, 352 (2014) 91–98.
- [33] B. Madhu, S. Ashwini, B. Shruthi, B. Divyashree, A. Manjunath, H. Jayanna, Structural, dielectric and electromagnetic shielding properties of Ni–Cu nanoferrite/PVP composites, *Mater. Sci. Eng. B.*, 186 (2014) 1–6.
- [34] E.E. Ateia, A.A. El-Bassuony, G. Abdelatif, F.S. Soliman, Novelty characterization and enhancement of magnetic properties of Co and Cu nanoferrites, *J. Mater. Sci.: Mater. Electron.*, 28 (2017) 241–249.
- [35] M. Trchová, J. Stejskal, Polyaniline: The infrared spectroscopy of conducting polymer nanotubes (IUPAC Technical Report), *Pure Appl. Chem.*, 83 (2011) 1803–1817.
- [36] R. Al-Oweini, H. El-Rassy, Synthesis and characterization by FTIR spectroscopy of silica aerogels prepared using several Si (OR) 4 and R'' Si (OR) 3 precursors, *J. Molec. Struct.*, 919 (2009) 140–145.
- [37] C. Hu, Y. Tang, C.Y. Jimmy, P.K. Wong, Photocatalytic degradation of cationic blue X-GRL adsorbed on TiO₂/SiO₂ photocatalyst, *Appl. Catal. B: Environ.*, 40 (2003) 131–140.